as those of the ⟨100⟩ valleys in Si and the ⟨111⟩ valleys in Ge. For Si, $\Xi_u = 9.2$ eV and $\Xi_d = -1.4$ eV, and, for Ge, $\Xi_u = 19.2$ eV and $\Xi_d = -10.5$ eV.[7,11–15]

These deformation potentials for the ⟨100⟩ valleys in GaAs ($\Xi_u = 16.8$ eV and $\Xi_d = -5.1$ eV) have been inserted into Conwell's[4] Eqs. (4.2) and (4.4) to calculate the electron mobility due to acoustic phonon scattering for electrons in the ⟨100⟩ valleys. The calculated lattice mobility is $\mu_L = 600$ cm²/V sec. This mobility was combined with the mobility limited by other scattering mechanisms to obtain a total mobility for electrons in the ⟨100⟩ valleys of $\mu_2 = 120$ cm²/V sec. This value is in agreement with the measured ⟨100⟩ electron mobility, 110 cm²/V sec.[21]

V. CONCLUSIONS

The electrical-resistivity measurements in GaAs as a function of temperature and uniaxial stress reveal two distinct types of behavior depending upon the source of the GaAs crystals. The two types of behavior are the limiting cases for GaAs in which the electrical properties are dominated by (1) a high concentration of deep-level impurities and traps, and (2) a moderate concentration of shallow-level impurities which remained completely ionized in these experiments.

The resistivity and Gunn-effect threshold measurements as a function of uniaxial stress provide experimental evidence that the ⟨100⟩ or X_1 valleys are the secondary conduction-band valleys in GaAs. Utilizing the recently measured value for $\Delta\mathcal{E} = 0.33$ eV,[25,26] the ratio of the densities of states is $N_2/N_1 = 40$ and the deformation potential for the ⟨100⟩ valleys are $\Xi_u^1 = 16.8$ eV/(unit strain), $\Xi_d^1 = -5.1$ eV/(unit strain) and, for the ⟨000⟩ valley, $\Xi_d^0 = 7.8$ eV/(unit strain). The value of Ξ_d^0 is in agreement with the value obtained by hydrostatic pressure measurements.[21] The calculated mobility of electrons in the ⟨100⟩ valleys is $\mu_2 = 120$ cm²/V sec which is also in agreement with the measured value of electron mobility[21] in the ⟨100⟩ valleys.

ACKNOWLEDGMENT

This work was supported by the Advanced Research Projects Agency through the Center for Materials Research at Stanford University. The authors wish to thank J. W. Allen, G. F. Day, F. Herman, and L. W. James for many helpful discussions.

PHYSICAL REVIEW B VOLUME 1, NUMBER 4 15 FEBRUARY 1970

Optical Double Resonance in Solids

YIZHAK YACOBY
Microwave Division, Department of Physics, Hebrew University, Jerusalem, Israel
(Received 1 April 1969)

Nonlinear interaction of two electromagnetic beams with a semiconducting or insulating crystal is considered under the following conditions: The photon energy $\hbar\Omega$ of an intense laser beam is equal to the gap between two conduction bands $\hbar\Omega_{32}$ at certain points in the crystal momentum space. The photon energy $\hbar\omega$ of a relatively weak beam is approximately equal to the gap between the valence band and one of the conduction bands $\hbar\Omega_{21}$ at the same points in crystal momentum space. These conditions are referred to as double resonance. A theory is developed for two nonlinear effects: (1) the change of the dielectric coefficient of the crystal at frequency ω caused by the Ω perturbation; and (2) the generation of a parametric beam at frequency $\omega+\Omega$. An interesting result of the theory is that both effects are very sensitive to the conditions at the point of contact of the surfaces of constant Ω_{31} and Ω_{21} in K space. The effects obtained when $\partial\Omega_{31}/\partial K_\perp$ and $\partial\Omega_{21}/\partial K_\perp$ have the same sign are much smaller than those obtained when they have opposite signs. ($K_\perp$ is the component of $\mathbf{K}$ perpendicular to the surfaces at the point of contact.) This phenomenon is explained in terms of combined electronic and electromagnetic states. Possible applications of these effects to the investigation of the band structure of solids are discussed. In particular, it is shown that measurements of double-resonance effects will yield information about the band structure at noncritical points in the Brillouin zone.

I. INTRODUCTION

IN recent years, several new optical methods were developed for the investigation of the band structure of solids. Methods which were found very useful in this respect are the electroabsorptance,[1] electroreflectance,[2] piezoreflectance,[3] and others known, in general, as the differential optical methods. These methods consist of measuring the variation in an optical property of the crystal, such as absorption or reflection coefficients, caused by the variation of a parameter, such as an

[1] A. Frova, P. Handler, F. A. Germano, and D. E. Aspnes, Phys. Rev. **145**, 575 (1966); Y. Yacoby, *ibid.* **142**, 445 (1966).

[2] B. O. Seraphin, Phys. Rev. **140**, A1716 (1965); M. Cardona, K. L. Shaklee, and F. H. Pollak, *ibid.* **154**, 696 (1967).

[3] M. Garfinkel, J. J. Tiemann, and W. E. Engeler, Phys. Rev. **148**, 695 (1966).

applied electric field or stress. The spectrum of the change in the optical property exhibits in most cases well-defined structures which are associated with the van Hove critical points in the Brillouin zone.

Two-photon absorption is developing into another method for the investigation of band structure. It essentially consists of applying a laser and a monochromatic beam to a crystal, so that the sum of their photon energies is approximately equal to the minimum energy gap in the material. Then, the absorption of the monochromatic beam, induced by the laser radiation, is measured as a function of the photon energy of the monochromatic beam. The theory for two-photon absorption has been worked out in detail including the case of excitons[4] at different levels of excitation. Measurements of two-photon spectra have been carried out in several materials,[5] and in many cases the results agree with the theory. The information provided by two-photon absorption spectra is complementary to the information obtained from the measurement of one-photon processes. The reason is that the selection rules for one-photon transitions are different from those of two-photon transitions. However, both methods suffer from the same difficulty, namely, the inability to resolve with ease different absorption processes.

A feature common to the one- and two-photon absorption and reflection methods, and to the differential optical methods, is that they only give useful information about the van Hove critical points in the Brillouin zone. The value of the absorption or reflection coefficients, at photon energies other than those corresponding to gaps at the critical points, depend on the properties of the material over a complete surface in K space. Consequently, band-structure calculations cannot be experimentally checked at noncritical points.

In this work, we shall show that measurements of nonlinear optical effects, under conditions of double resonance, may provide information that can be directly compared with theoretical band-structure models of solids, at points in the Brillouin zone which are not critical, but located along lines of high symmetry. By double resonance we mean that two electromagnetic perturbations are simultaneously applied to a material system, and the photon energy of one is equal to the energy difference between a pair of states, while the photon energy of the other is equal to the energy difference between one of these levels and a third one. The theoretical treatment of double-resonance effects is slightly different from the treatment of other nonlinear optical effects, mainly because the displacement currents in the first case cannot be expressed in power series of the electric fields. One must, therefore, treat this problem to all powers of the electric fields of strong laser beams. Fortunately, however, the treatment is considerably simplified because very few matrix elements are accompanied with resonant denominators and in most cases, the rest may be neglected. Such a treatment of nonlinear interaction of radiation with matter under double-resonance conditions has been carried out by several authors[6] for systems with discrete energy levels. These effects have been observed in the microwave domain, but to our knowledge have not yet been observed when both electromagnetic radiations are in the optical-frequency domain.

In this work, we consider nonlinear optical effects under conditions of double resonance in solids, where the energy levels are not discrete. Specifically, we consider the following case: Two electromagnetic radiations are applied to a semiconducting or insulating crystal at frequencies ω and Ω. The radiation with frequency Ω is taken to be an intense laser radiation, whereas the radiation with frequency ω is a weak radiation. We consider the existence of three bands—a full valence band and two empty conduction bands. The photon energies are assumed to be close to double resonance in a certain region in K space. To avoid absorption of the laser radiation by electronic transitions from valence to conduction band, we assume that $\hbar\Omega$ is smaller than the minimum energy gap between the valence band and the lower conduction band.

In Sec. II, we adopt the method of Javan and Szöke[6] for treating double-resonance effects to our particular conditions. We first obtain expressions for the density-matrix elements describing an electron with a given crystal momentum $\mathbf{K}$. Then, we express the contribution to the polarization current by an electron with crystal momentum $\mathbf{K}$ in terms of the density matrix. In Sec. III, we discuss the change of the polarization current with frequency equal to ω, caused by the Ω perturbation. Numerical computations are given, illustrating the different aspects of the results. The polarization current with frequency equal to $\omega+\Omega$ is treated in Sec. IV. This current produces a parametric electromagnetic beam. The different properties of this beam are illustrated numerically. In Sec. V, we discuss several experimental applications of double-resonance effects which are useful in the investigation of band structure of solids.

II. POLARIZATION CURRENT

The one-electron Hamiltonian for an electron in a solid in the presence of the perturbing radiations described in the Introduction is given by

$$H=(\mathbf{P}-e\mathbf{A}-e\mathbf{B})^2/2m+V. \quad (1)$$

[4] R. Braunstein, Phys. Rev. **125**, 475 (1962); R. Loudon, Proc. Phys. Soc. (London) **80**, 952 (1962); G. D. Mahan, Phys. Rev. **170**, 825 (1968).

[5] J. J. Hopfield and J. M. Worlock, Phys. Rev. **137**, A1455 (1965); D. Fröhlich and H. Mahr, Phys. Rev. Letters **16**, 895 (1966); D. Fröhlich and E. Schönherr, *ibid.* **19**, 1032 (1967); J. P. Hernandez and A. Gold, Phys. Rev. **156**, 26 (1967).

[6] S. Yatsiv, Phys. Rev. **113**, 1538 (1959); A. Javan and A. Szöke, *ibid.* **137**, A536 (1965).

Here **P** is the momentum operator, **A** and **B** are the vector potentials of the ω and Ω perturbations, respectively, and V is the periodic potential. Since we are interested in conditions which are close to double resonance, we shall neglect all terms in the density matrix which do not have resonant denominators. Thus, the only matrix elements of the Hamiltonian which contribute to the dominating terms in the density matrix are

$$H_{12}=(-eA_0/2m)\langle\Phi_1|\mathbf{P}\cdot\mathbf{U}|\Phi_2\rangle e^{i\omega t}=d_{12}e^{i\omega t}, \quad (2)$$

$$H_{23}=(-eB_0/2m)\langle\Phi_2|\mathbf{P}\cdot\mathbf{V}|\Phi_3\rangle e^{i\Omega t}=d_{23}e^{i\Omega t}. \quad (3)$$

Here Φ_1, Φ_2, and Φ_3 are the Bloch wave functions corresponding to the valence and to the lower and upper conduction bands, respectively, and **U** and **V** are unit vectors in the directions of the vectors **A** and **B**, respectively. Neglecting the momentum of the photons, the perturbing electromagnetic radiations couple states of the same **K** values. As a result of this perturbation, electron-hole pairs are produced which interact with phonons and make intraband transitions. Through these transitions, the electrons and holes reach the extrema of the bands, where they recombine. Let us now consider a given point in **K** space. We denote the matrix elements of the density operator, with respect to the Bloch states and with crystal momentum **K**, by ρ_{ij}. The equation which the matrix ρ satisfies is given by

$$i\hbar(d\rho/dt)=[H,\rho]+i\hbar I, \quad (4)$$

where

$$I=\begin{pmatrix}(1-\rho_{11})/\tau-I_1 & -\rho_{12}/T & -\rho_{13}/T\\ -\rho_{21}/T & -\rho_{22}/\tau+I_2 & -\rho_{23}/T\\ -\rho_{31}/T & -\rho_{32}/T & -\rho_{33}/\tau+I_3\end{pmatrix}. \quad (5)$$

Here τ is the diagonal relaxation time, which for simplicity is taken to be the same for all bands; similarly, T is the off-diagonal relaxation time. I_1 is equal to the number of holes which flow to the point **K** per unit time through intraband transitions. Similarly, I_2 and I_3 are the electronic flows to the points **K** within the two conduction bands.

We assume that the solutions to these equations have the following time dependences:

$$\begin{aligned}&\rho_{12}=\lambda_{12}e^{i\omega t}, \quad \rho_{13}=\lambda_{13}e^{i(\omega+\Omega)t},\\ &\rho_{23}=\lambda_{23}e^{i\Omega t}, \quad \rho_{11}=\lambda_{11},\\ &\rho_{22}=\lambda_{22}, \quad \rho_{33}=\lambda_{33},\end{aligned} \quad (6)$$

where λ_{ij} is time-independent. Substituting these expressions for the matrix elements in Eq. (4), we obtain a set of nine linear algebraic equations for λ_{ij},

$$[i(\omega-\Omega_{21})+T^{-1}]\lambda_{12}-i\hbar^{-1}d_{23}^*\lambda_{13}+i\hbar^{-1}d_{12}\lambda_{22}+i\hbar^{-1}d_{12}\bar{\lambda}_{11}=i\hbar^{-1}d_{12}, \quad (7a)$$

$$[i(\omega+\Omega-\Omega_{31})+T^{-1}]\lambda_{13}+i\hbar^{-1}d_{12}\lambda_{23}-i\hbar^{-1}d_{23}\lambda_{12}=0, \quad (7b)$$

$$[i(\Omega-\Omega_{32})+T^{-1}]\lambda_{23}+i\hbar^{-1}d_{12}^*\lambda_{13}+i\hbar^{-1}d_{23}(\lambda_{33}-\lambda_{22})=0, \quad (7c)$$

$$\bar{\lambda}_{11}\tau^{-1}-i\hbar^{-1}d_{12}\lambda_{12}^*+i\hbar^{-1}\lambda_{12}d_{12}^*=I_1, \quad (7d)$$

$$\lambda_{22}\tau^{-1}+i\hbar^{-1}d_{12}^*\lambda_{12}-i\hbar^{-1}d_{12}\lambda_{12}^*+i\hbar^{-1}d_{23}\lambda_{23}^*-i\hbar^{-1}d_{23}^*\lambda_{23}=I_2, \quad (7e)$$

$$\lambda_{33}\tau^{-1}+i\hbar^{-1}d_{23}^*\lambda_{23}-i\hbar d_{23}\lambda_{23}^*=I_3, \quad (7f)$$

where $\bar{\lambda}_{11}=1-\lambda_{11}$ and $\hbar\Omega_{21}$, $\hbar\Omega_{31}$, and $\hbar\Omega_{32}$ are the energy differences between the valence and lower conduction band, the valence and upper conduction band and between the lower and upper conduction bands, respectively. The other three equations are the complex conjugates of Eqs. (7a)–(7c). One can express λ_{ij} as a sum of four components,

$$\lambda_{ij}=\lambda_{ij}^{(1)}+\lambda_{ij}^{(2)}+\lambda_{ij}^{(3)}+\lambda_{ij}^{(4)}, \quad (8)$$

where $\lambda_{ij}^{(1)}$ is the solution of Eqs. (7a)–(7f) with the right-hand side of these equations except Eq. (7a) taken equal to zero; similarly $\lambda_{ij}^{(2)}$ is the solution with the right-hand side of the above equations except Eq. (7d) taken equal to zero, etc.

Let us first solve the equation for $\lambda_{ij}^{(1)}$. From Eq. (7f) one obtains

$$\lambda_{33}^{(1)}\tau^{-1}=i\hbar^{-1}(d_{23}\lambda_{23}^{(1)*}-d_{23}^*\lambda_{23}^{(1)}). \quad (9)$$

Adding Eqs. (7e) and (7f), the following equation results:

$$\lambda_{22}^{(1)}\tau^{-1}+\lambda_{33}^{(1)}\tau^{-1}=i\hbar^{-1}(d_{12}\lambda_{12}^{(1)*}-d_{12}^*\lambda_{12}^{(1)}). \quad (10)$$

Since $\lambda_{22}^{(1)}$ and $\lambda_{33}^{(1)}$ are positive, it is clear that

$$\lambda_{22}^{(1)}+\lambda_{33}^{(1)}>\lambda_{33}^{(1)}.$$

Thus, $|d_{12}\lambda_{12}^{(1)*}|$ is of the same order of magnitude as $|d_{23}\lambda_{23}^{(1)}|$. However, since $|d_{23}|\gg|d_{12}|$, one finds that

$$|d_{12}\lambda_{23}^{(1)}|\ll|d_{23}\lambda_{12}^{(1)}|. \quad (11)$$

Using this inequality in Eq. (7b), one obtains an expression for $\lambda_{13}^{(1)}$ in terms of $\lambda_{12}^{(1)}$,

$$\lambda_{13}^{(1)}=i\hbar^{-1}d_{23}\lambda_{12}^{(1)}[i(\omega+\Omega-\Omega_{31})+T^{-1}]^{-1}. \quad (12)$$

Substituting this expression in Eq. (7a) and neglecting $\bar{\lambda}_{11}^{(1)}$ and $\lambda_{12}^{(1)}$ with respect to unity, one obtains an explicit expression for $\lambda_{12}^{(1)}$,

$$\lambda_{12}^{(1)}=\frac{id_{12}\hbar^{-1}}{[i(\omega-\Omega_{21})+T^{-1}]+|d_{23}|^2/\hbar^2[i(\omega+\Omega-\Omega_{31})+T^{-1}]}. \quad (13)$$

One can now, by proper manipulation of the equations, obtain expressions for $\lambda_{23}^{(1)}$ and $\lambda_{33}^{(1)}$. These expressions are not presented because these density-matrix elements will not be used later.

As previously explained the current I_1 is a current of holes, which flows to the point **K** under consideration through interactions with lattice vibrations. The evaluation of I_1, I_2, and I_3 is beyond the scope of this work. Here, we shall only discuss which of the elements λ_{ij} is influenced by these currents.

The production of a hole or an electron must be associated with a transition from the valence band. Thus, it must be accompanied by the absorption of a photon $\hbar\omega$ of the weak beam. As a result, all three currents will be very small compared to τ^{-1}. Taking into account that the coupling between the valence and conduction bands is weak, whereas the coupling between the two conduction bands is strong, one can easily arrive at the following results:

(a) $\lambda_{ij}^{(2)} \ll \lambda_{ij}^{(1)}$, for i or j different from 1. $\bar{\lambda}_{11}^{(2)}$ may be comparable to or even larger than $\bar{\lambda}_{11}^{(1)}$;

(b) $\lambda_{ij}^{(3)} \ll \lambda_{ij}^{(1)}$, for all pairs of i, j except for the pairs (2,2); (2,3); (3,2); and (3,3); and

(c) $\lambda_{ij}^{(4)} \ll \lambda_{ij}^{(1)}$, for all pairs of i, j except for the pairs (2,2); (2,3); (3,2); and (3,3).

The only matrix elements which will be used later are ρ_{12} and ρ_{13}. These matrix elements as shown here are approximately independent of I_1, I_2, and I_3. All the other matrix elements can be easily obtained. However, since they are not used later, they are not presented explicitly.

We can now set forth to obtain expressions for the nonlinear polarization current. We denote the polarization vector of a single electron with a wave number **K** by $\mathfrak{y}_0$. The expectation value of $\mathfrak{y}_0$ is given by

$$\langle \mathfrak{y}_0 \rangle = \mathrm{Tr}(\rho \mathfrak{y}_0). \tag{14}$$

A more explicit form of this expression is

$$\langle \mathfrak{y}_0 \rangle = (\rho_{11}\mathfrak{y}_{11}+\rho_{22}\mathfrak{y}_{22}+\rho_{33}\mathfrak{y}_{33})+(\rho_{12}\mathfrak{y}_{21}+\rho_{21}\mathfrak{y}_{12}) +(\rho_{13}\mathfrak{y}_{31}+\rho_{31}\mathfrak{y}_{13})+(\rho_{23}\mathfrak{y}_{32}+\rho_{32}\mathfrak{y}_{23}), \tag{15}$$

where $\mathfrak{y}_{ij}$ are the matrix elements of $\mathfrak{y}_0$, with respect to the Bloch functions at the particular **K** value which is being considered. The first term in the brackets is time-independent, whereas the other three terms are time-dependent with frequencies ω, $\omega+\Omega$, and Ω, respectively. Thus, $d\langle \mathfrak{y}_0 \rangle/dt$ is given by

$$d\langle \mathfrak{y}_0 \rangle/dt = i\omega(\rho_{12}\mathfrak{y}_{21}-\rho_{21}\mathfrak{y}_{12})+i(\omega+\Omega) \times(\rho_{13}\mathfrak{y}_{31}-\rho_{31}\mathfrak{y}_{13})+i\Omega(\rho_{23}\mathfrak{y}_{32}-\rho_{32}\mathfrak{y}_{23}); \tag{16}$$

$\mathfrak{y}_{ij}$ can also be expressed in the form

$$\mathfrak{y}_{ij} = -[eh/im(E_i-E_j)]\mathbf{P}_{ij}. \tag{17}$$

Substituting this expression in Eq. (16), one obtains

$$\mathbf{J}_0 = \frac{d\langle \mathfrak{y}_0 \rangle}{dt} = -\frac{eh}{m}\frac{\omega}{E_2-E_1}(\rho_{12}\mathbf{P}_{21}+\rho_{21}\mathbf{P}_{12}) -\frac{eh}{m}\frac{\omega+\Omega}{E_3-E_1}(\rho_{13}\mathbf{P}_{31}+\rho_{31}\mathbf{P}_{13}) -\frac{eh}{m}\frac{\Omega}{E_3-E_2}(\rho_{23}\mathbf{P}_{32}+\rho_{32}\mathbf{P}_{23}). \tag{18}$$

The first term in this expression is the polarization current with frequency equal to ω. Since this current is proportional to the electric field at this frequency, one may define a conductivity σ which is the ratio between the polarization current and the electric field with frequency ω. This conductivity is related to the complex expansion coefficient γ of the ω beam in the crystal through the equation $\gamma=(\sigma j\omega\eta)^{1/2}$, where η is the permeability constant. For reasons of convenience, we shall discuss only the polarization current rather than the expansion coefficient. The second term is a polarization current with a frequency equal to $\omega+\Omega$. This current produces a parametric electromagnetic radiation. The third term is the polarization current with frequency equal to Ω. This current causes the absorption and reflection of the beam with frequency Ω. We shall not evaluate the third term because the relative change in this polarization current, caused by the ω perturbation, is extremely small and very difficult to measure.

The total polarization current is obtained by integrating $\mathbf{J}_0$ over K space. As previously mentioned, the major contribution to the integral will come from regions in K space in which almost double-resonance conditions exist. Unlike gases, where double-resonance conditions take place for all atoms at practically the same exciting energy, double-resonance conditions in solids do not exist at all points in K space for the same exciting energies. The points at which double-resonance conditions are satisfied are the points common to the two surfaces $\Omega_{21}(\mathbf{K})-\omega=0$ and $\Omega_{31}(\mathbf{K})-(\omega+\Omega)=0$.

In the general case, at the most the two surfaces cut each other along lines. For particular values of ω and Ω, the two surfaces just touch, and for other values, they have no points in common. There is one case in which the two surfaces may coincide. This is the case of surfaces around $\mathbf{K}=0$ in a crystal with full cubic symmetry. In this case, the surfaces are spheres which coincide when $\Omega_{21}-\omega=0$ and $\Omega_{31}-(\omega+\Omega)=0$. Both the general case and the case of two spherical surfaces will be discussed in detail in Sec. III.

III. POLARIZATION CURRENT WITH FREQUENCY EQUAL TO ω

An explicit expression for the polarization with frequency equal to ω can be obtained by substituting expressions (6) and (13) for ρ_{12} and ρ_{21} in Eq. (18) and integrating in K space. As pointed out previously, $\lambda_{12}^{(2)}$, $\lambda_{12}^{(3)}$, and $\lambda_{12}^{(4)}$ are negligible compared to $\lambda_{12}^{(1)}$, and similarly, the changes caused by the Ω perturbation in $\lambda_{12}^{(2)}$, $\lambda_{12}^{(3)}$, and $\lambda_{12}^{(4)}$ are negligible compared to the change in $\lambda_{12}^{(1)}$. Therefore, the dielectric current

$\mathbf{J}_\omega$ is given by

$$\mathbf{J}_\omega=\frac{1}{4\pi^3}\int d^3K\frac{e^2\hbar\omega}{2m^2\hbar(E_2-E_1)}\Bigg(\frac{2T[S_{12}-\xi_{23}S_{13}/(S_{13}^2+1)]}{[S_{12}-\xi_{23}S_{13}/(S_{13}^2+1)]^2+[1+\xi_{23}/(S_{13}^2+1)]^2}\,\mathrm{Re}[(\mathbf{A}\cdot\mathbf{P}_{12})\mathbf{P}_{21}]$$
$$-\frac{2T[1+\xi_{23}/(S_{13}^2+1)]}{[S_{12}-\xi_{23}S_{13}/(S_{13}^2+1)]^2+[1+\xi_{23}/(S_{13}^2+1)]^2}\,\mathrm{Im}[(\mathbf{A}\cdot\mathbf{P}_{12})\cdot\mathbf{P}_{21}]\Bigg),\quad(19)$$

where

$$\xi_{23}=|d_{23}|^2T^2/\hbar^2,\quad S_{12}=(\omega-\Omega_{21})T,$$
$$S_{13}=(\omega+\Omega-\Omega_{31})T.\quad(20)$$

The integrand in Eq. (19) is too complicated for the integral over K space to be carried out in the general form. We shall, therefore, present at first a qualitative discussion which will give some insight into the kind of results that one may expect, and then present several numerical examples. According to our assumptions, the ω perturbation is weak. Thus, J_ω is linear in the ω perturbation. As a result of this, the two components of $\mathbf{J}_\omega$, $\mathbf{J}_{\omega c}$, and $\mathbf{J}_{\omega s}$ are related to each other through the Kramers-Kronig relation. We shall, therefore, confine our qualitative discussion to the second term $\mathbf{J}_{\omega s}$ in Eq. (19).

We notice that in the absence of the Ω perturbation, the expression under consideration has a resonant denominator with its peak at $S_{12}=0$, i.e., at $\omega=\Omega_{21}$. The effect of the Ω perturbation for a given value of S_{13} is to shift and broaden this resonance. The sign of the shift is positive or negative, depending on the sign of S_{13}. The effect of such a shift will be most pronounced in the vicinity of the band extrema because there the change in the density of states is strongest. Several numerical calculations of the change in the polarization current caused by the Ω perturbation in the vicinity of the band extrema have been carried out.

For simplicity we confine ourselves to the following case: (a) The bands are not degenerate; (b) $\mathbf{U}$ and $\mathbf{V}$ are both in a direction along which the crystal has twofold reflection symmetry; and (c) the effective masses are taken to be scalar quantities. In this simplified case, $[(\mathbf{A}\cdot\mathbf{P}_{12})\mathbf{P}_{21}]=\mathbf{A}_0e^{i\omega t}|P_{12}|^2$. One can express S_{12} and S_{13} in the following way:

$$S_{12}=(\omega-\Omega_{210})T-\gamma_{21}K^2,$$
$$S_{13}=(\omega+\Omega-\Omega_{310})T-\gamma_{13}K^2,\quad(21)$$

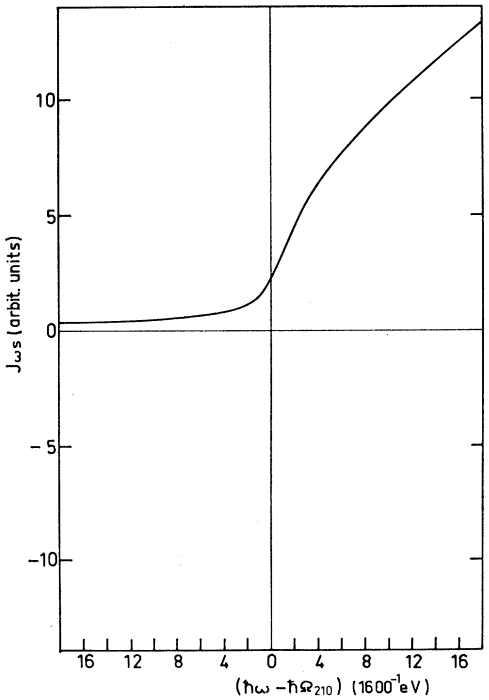

FIG. 1. $J_{\omega s}$ as a function of $(\hbar\omega-\hbar\Omega_{210})$, computed with $T=10^{-12}$ sec. Horizontal coordinate: 1 unit $=1600^{-1}$ eV. Vertical coordinate: arbitrary.

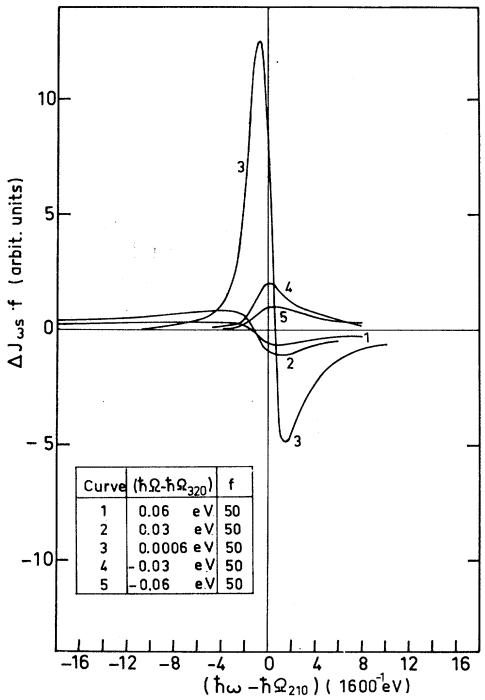

FIG. 2. $\Delta J_{\omega s}$ as a function of $(\hbar\omega-\hbar\Omega_{210})$ for different values of $(\hbar\Omega-\hbar\Omega_{320})$ computed under the following conditions: $T=10^{-12}$ sec; $\gamma_{13}/\gamma_{12}=0.3$; $\xi_{23}=2$ (the corresponding intensity of the Ω perturbation is approximately equal to 2×10^8 W/cm^2). Horizontal coordinate: 1 unit $=1600^{-1}$ eV. Vertical coordinate: The units of $\Delta J_{\omega s}\times f$ are equal to the vertical units in Fig. 1.

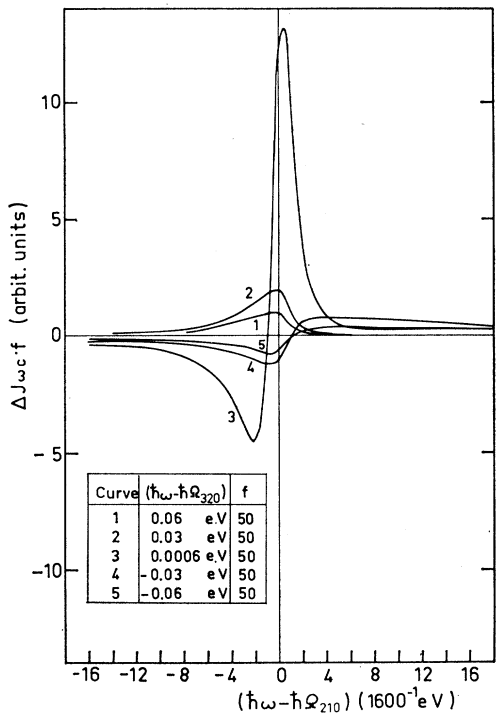

FIG. 3. $\Delta J_{\omega c}$ as a function of $(\hbar\omega - \hbar\Omega_{210})$ for different values of $(\hbar\Omega - \hbar\Omega_{320})$, computed under the following conditions: $T = 10^{-12}$ sec; $\gamma_{13}/\gamma_{12} = 0.3$; $\xi_{23} = 2$ (the corresponding intensity of the Ω beam is approximately equal to 2.10^8 W/cm^2). Horizontal coordinate: 1 unit $= 1600^{-1}$ eV. Vertical coordinate: The units of $\Delta J_{\omega c} \times f$ are equal to the vertical units in Fig. 1.

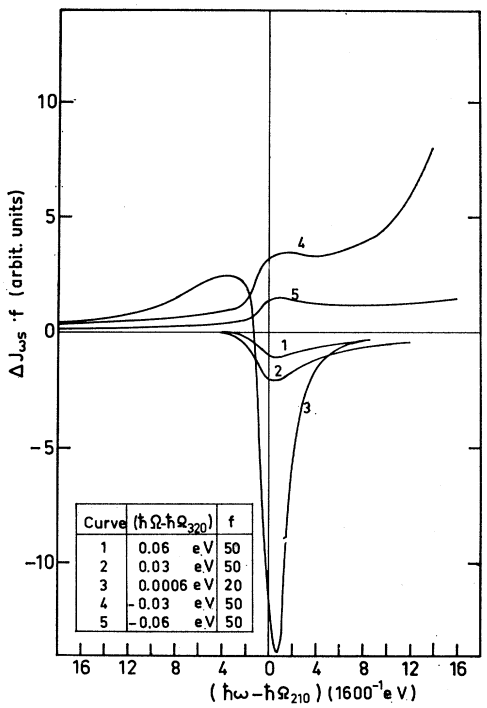

FIG. 4. $\Delta J_{\omega s}$ as a function of $(\hbar\omega - \hbar\Omega_{210})$ for different values of $(\hbar\Omega - \hbar\Omega_{320})$, computed under the following conditions: $T = 10^{-12}$ sec; $\gamma_{13}/\gamma_{12} = -0.3$; $\xi_{23} = 2$ (the corresponding intensity of the beam is approximately equal to 2.10^8 W/cm^2). Horizontal coordinate: 1 unit $= 1600^{-1}$ eV. Vertical coordinate: The units of $\Delta J_{\omega c} \times f$ are equal to the vertical units in Fig. 1.

where

$$\gamma_{12} = \tfrac{1}{2}(m_1^{*-1} + m_2^{*-1})\hbar T$$

and (22)

$$\gamma_{13} = \tfrac{1}{2}(m_1^{*-1} + m_3^{*-1})\hbar T,$$

and m_1^*, m_2^*, and m_3^* are the effective masses of the holes in the valence band and the electrons in the conduction bands, respectively. Notice that m_3^* may also be negative. Substituting these expressions for S_{12} and S_{13} in Eq. (19), we find that the integrand is a function of $|K|$ alone. One can then integrate first over a surface of constant K and then with respect to $|K|$. The integrand in the integral with respect to $|K|$ is a ratio between two polynomials in $|K|$ and can therefore be integrated exactly. We chose to perform the integration by evaluating the residues in the complex plane with the aid of a computer. The change in the polarization current caused by the Ω perturbation has been evaluated as a function of $\hbar\omega$ with $\hbar\Omega$ as a parameter. We performed this calculation for a positive and for a negative combined effective mass of the valence and upper conduction bands.

The polarization current $\mathbf{J}_{\omega s}$ caused by the ω perturbation only is given in Fig. 1. The other component of the polarization current depends on the whole band structure and cannot be evaluated in a general form. The change in the polarization current $\Delta\mathbf{J}_{\omega s}$ caused by the Ω perturbation for positive γ_{13} is shown in Fig. 2. $\Delta\mathbf{J}_{\omega s}$ for negative γ_{13} is shown in Fig. 4. The spectra of $\Delta J_{\omega c}$ are shown in Figs. 3 and 5 for positive and negative γ_{13}, respectively. The particular conditions under which the calculations have been carried out are given in tables which appear in the respective figures. As expected, $\Delta\mathbf{J}_\omega$ attains its largest value when $\hbar\omega$ is very close to the minimum energy gap $\hbar\Omega_{210}$. When $\hbar\Omega$ is not equal to $\hbar\Omega_{320}$, $\Delta\mathbf{J}_{\omega s}$ and $\Delta\mathbf{J}_{\omega c}$ have the form of rather sharp peaks with a width of about 3 meV. When $\hbar\Omega > \hbar\Omega_{320}$, $\Delta J_{\omega s}$ is negative, corresponding to an effective increase in the energy gap. The opposite happens when $\hbar\Omega < \hbar\Omega_{320}$. For values of $\hbar\Omega$ very close or equal to $\hbar\Omega_{320}$, $\Delta\mathbf{J}_\omega$ is extremely large. Under the conditions of the computation, $\Delta\mathbf{J}_{\omega s}$ reaches values such that $|\Delta\mathbf{J}_{\omega s}|/|\mathbf{J}_{\omega s}| \cong 0.3$. In the case of negative combined effective mass (Fig. 4) and $\hbar\Omega < \hbar\Omega_{320}$, the value of $\Delta\mathbf{J}_\omega$ starts increasing again for $\hbar\omega > \hbar\Omega_{210}$. This effect is associated with a double resonance which takes place for a value of $\hbar\omega$ larger than $\hbar\Omega_{210}$. Notice that this effect does not appear under similar conditions in the case of positive combined effective mass, $\gamma_{13} > 0$, shown in Fig. 2. This behavior will be explained later in this section.

The dependence of $\Delta\mathbf{J}_\omega$ on the intensity of the Ω beam enters through ξ_{23}, defined in Eq. (20). For values of ξ_{23} much smaller than unity, $\Delta\mathbf{J}_\omega$ is found to be propor-

tional to ξ_{23}, which is proportional to the intensity of the Ω radiation. However, when ξ_{23} is larger than unity, deviations from the linear dependence are expected. An example of the dependence of $\Delta\mathbf{J}_{\omega s}$ on ξ_{23} is given in Fig. 6. Here, $\Delta J_{\omega s}$ is given as a function of $\hbar\omega$ for different values of ξ_{23}.

Let us now consider the case in which double-resonance conditions exist over a sphere in $\mathbf{K}$ space. As pointed out, we would expect rather strong effects to appear in this case. The component of the polarization current with frequency ω is given by

$$\mathbf{J}_\omega=\frac{1}{4\pi^3}\int_0^{2\pi}d\varphi\int_0^{\pi}\sin\theta\,d\theta\int_0^{\infty}K^2\mathbf{J}_{0\omega}\,dK. \quad (23)$$

$\mathbf{J}_{0\omega}$ depends on ω through S_{12} and S_{13} only. S_{12} and S_{13} depend on $|K|$, but are approximately independent of θ and φ. On the other hand, ξ_{23} and $[(\mathbf{A}\cdot\mathbf{P}_{12})\mathbf{P}_{21}]$ do not depend appreciably on $|K|$, but do depend on θ and φ. The result of the integration with respect to these two variables is a function of the angle between $\mathbf{U}$ and $\mathbf{V}$ and of the symmetry properties of the bands involved. $\mathbf{J}_{0\omega}$ is approximately proportional to ξ_{23} when $\xi_{23}<1$. Thus, in this case the dependence of $\mathbf{J}_\omega$ on ω will be the same as that of

$$\int_0^{\infty}J_{0\omega}K^2\,dK.$$

Thus, in order to obtain the dependence of $\mathbf{J}_\omega$ on ω, it is sufficient to consider the integral with respect to $|K|$ only.

Before evaluating this integral numerically, let us analyze it under the simplifying condition that $T\to\infty$. We once again limit our discussion to $\mathbf{J}_{\omega s}$. A more explicit expression for $\mathbf{J}_{\omega s}$ is needed for the present discussion:

$$\mathbf{J}_{\omega s}=-\frac{1}{4\pi^3}\int_0^{2\pi}d\varphi\int_0^{\pi}\sin\theta\,d\theta\frac{e^2\hbar\omega}{2m^2\hbar(E_2-E_1)}\mathrm{Im}[(\mathbf{A}\cdot\mathbf{P}_{12})\cdot\mathbf{P}_{21}]\int_0^{\infty}dK\Bigg[\frac{2}{T}\Bigg(1+\frac{|d_{23}|^2}{\hbar^2[(\omega+\Omega-\Omega_{31})^2+T^{-2}]}\Bigg)\Bigg/$$

$$\Bigg\{\Bigg((\omega-\Omega_{21})-\frac{|d_{23}|^2(\omega+\Omega-\Omega_{31})}{\hbar^2[(\omega+\Omega-\Omega_{31})^2+T^{-2}]}\Bigg)^2+\Bigg[\frac{1}{T}\Bigg(1+\frac{|d_{23}|^2}{\hbar^2[(\omega+\Omega-\Omega_{31})^2+T^{-2}]}\Bigg)\Bigg]^2\Bigg\}\Bigg]. \quad (24)$$

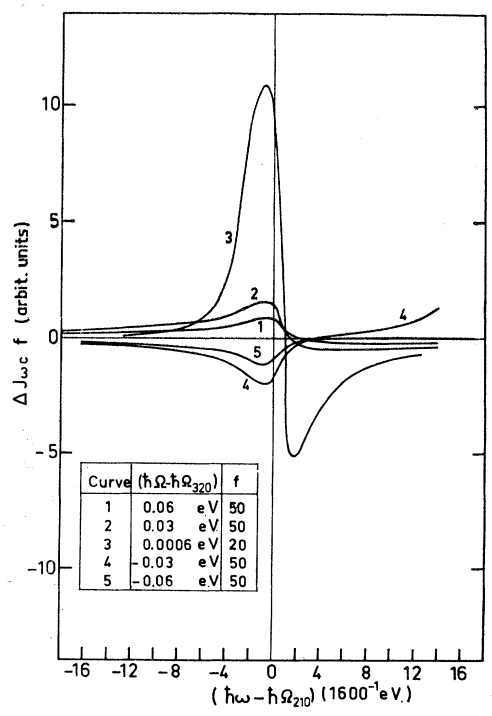

FIG. 5. $\Delta J_{\omega c}$ as a function of $(\hbar\omega-\hbar\Omega_{210})$ for different values of $(\hbar\Omega-\hbar\Omega_{320})$, computed under the following conditions: $T=10^{-12}$ sec; $\gamma_{13}/\gamma_{12}=-0.3$; $\xi_{23}=2$ (the corresponding intensity of the beam is approximately equal to 2.10^8 W/cm^2). Horizontal coordinate: 1 unit $=1600^{-1}$ eV. Vertical coordinate: The units of $\Delta J_{\omega c}\times f$ are equal to the vertical units in Fig. 1.

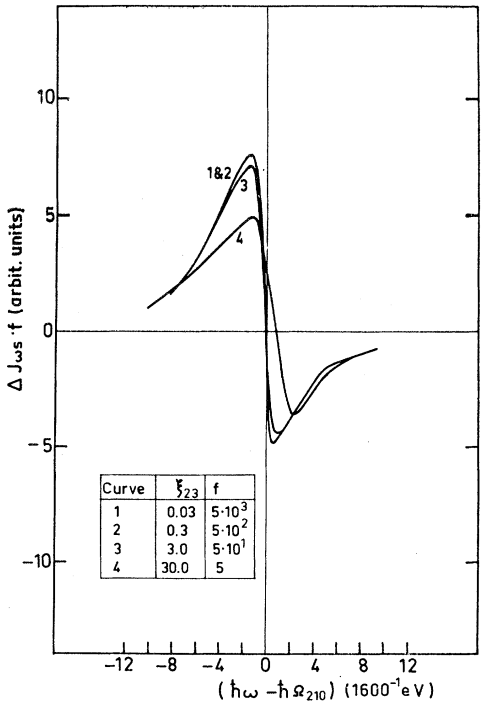

FIG. 6. $\Delta J_{\omega s}$ as a function of $(\hbar\omega-\hbar\Omega_{210})$ for different values of ξ_{23}, computed under the following conditions: $T=10^{-12}$ sec; $\gamma_{13}/\gamma_{12}=0.3$; $(\hbar\Omega-\hbar\Omega_{320})=6$ meV. Horizontal coordinate: 1 unit $=1600^{-1}$ eV. Vertical coordinate: The units of $\Delta J_{\omega s}\times f$ are equal to the vertical units in Fig. 1.

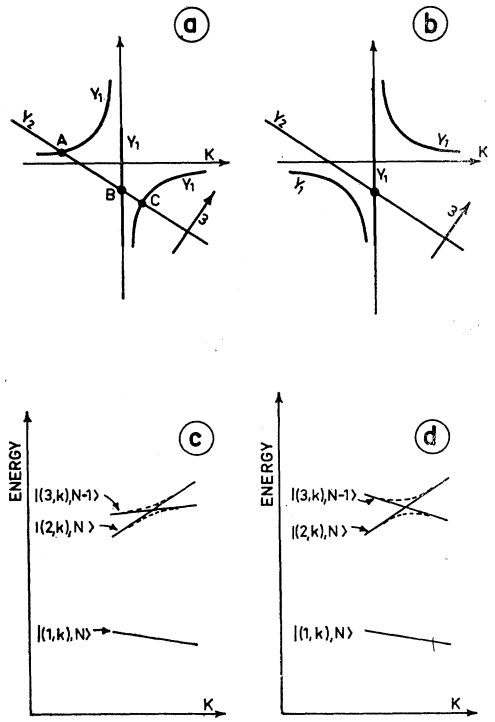

FIG. 7. (a) Determination of the poles of $J_{0\omega s}$ for $\gamma_{13}/\gamma_{12}>0$. (b) Determination of the poles of $J_{0\omega s}$ for $\gamma_{13}/\gamma_{12}<0$. (c) Composite bands of an electron and the electromagnetic oscillator with frequency equal to Ω for $\gamma_{13}/\gamma_{12}>0$. (d) Composite bands of an electron and the electromagnetic oscillator with frequency equal to Ω for $\gamma_{13}/\gamma_{12}<0$.

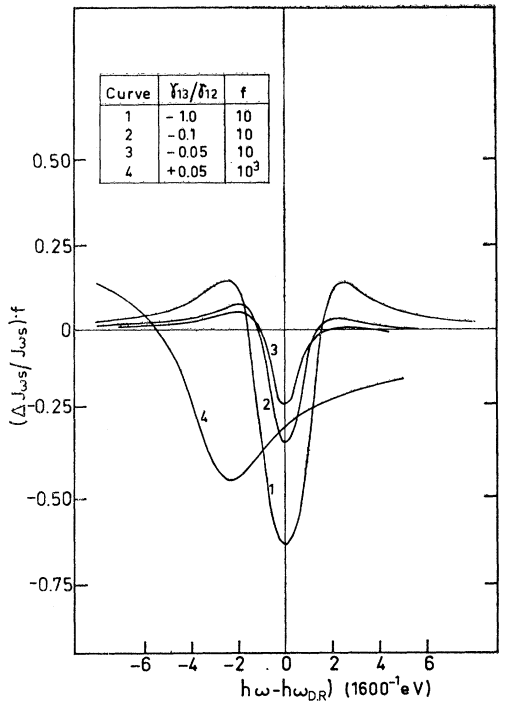

FIG. 8. $\Delta J_{\omega s}/J_{\omega s}$ as a function of the deviation of $\hbar\omega$ from its double resonance value $\hbar\omega_{DR}$ computed under the following conditions: $T=10^{-12}$ sec. $\hbar\omega_{DR}-\hbar\Omega_{210}=30$ meV; $\xi_{23}=0.5$. (The corresponding intensity of the Ω perturbation is approximately equal to 5×10^7 W/cm^2.) Horizontal coordinate: 1 unit $=1600^{-1}$ eV.

For the purpose of this discussion, we assume that the dependence of $\omega-\Omega_{21}$ and $\omega+\Omega-\Omega_{31}$ on K is linear in the vicinity of the double resonance. Notice now that the second term in the denominator approaches zero provided $\omega+\Omega-\Omega_{31}\neq0$. Therefore, zeros of the first term in the denominator determine the poles of the integrand. The zeros may be found from the intersection of the curve

$$Y_1=|d_{23}|^2(\omega+\Omega-\Omega_{31})/\hbar^2[(\omega+\Omega-\Omega_{31})^2+T^{-2}]$$

and the straight line $Y_2=\omega-\Omega_{21}$. These curves are shown for positive combined effective mass of bands 1 and 3 in Fig. 7(a) and for negative combined effective mass in Fig. 7(b). For simplicity, we assume that $\omega+\Omega$ is constant but consider different values of ω. As ω varies, the curve Y_1 remains unchanged, but the straight line shifts. In the first case [Fig. 7(a)] Y_1 and Y_2 intersect at three points A, B, and C. A and C are poles of the integrand, whereas at B, $\omega+\Omega-\Omega_{31}=0$, causing the integrand to vanish at this point. In the second case, the behavior is completely different. There is a certain range of values of ω for which the integrand does not have poles on the real K axis and because $T\to\infty$ the integral vanishes. The integral in the first case can also be easily performed because the contribution comes only from values of K in the vicinity of the poles. The interesting point is that the result is found to be independent of ω. The sharp decrease in the polarization current in the second case means that the transition from the valence band becomes impossible for a certain range of values of ω.

This behavior can be better understood in another way, used by Barrat and Cohen-Tannoudji[7] in discussing double resonance in systems with discrete energy levels. Consider composite electron-phonon states $|(n,\mathbf{K}),N\rangle$, where n designates the number of the band, $\mathbf{K}$ the wave number of the electron, and N the number of the photons of the electromagnetic oscillator with frequency Ω. In a transition from the valence band $|(1,K),N\rangle$, the electron may absorb a photon $\hbar\omega$ and go to the state $|(2,\mathbf{K}),N\rangle$, or absorb two photons $\hbar(\omega+\Omega)$, and thus be found in the compound state $|(3,\mathbf{K}),N-1\rangle$. A schematic plot of these energy levels as a function of K for a positive combined effective mass of bands 1 and 3 is shown in Fig. 7(c). The solid lines describe the energy levels if one neglects the interaction between the states $|(2,\mathbf{K})N\rangle$ and $|(3,\mathbf{K}),N-1\rangle$. However, these two states are not eigenstates of the combined Hamiltonian, and there is a term in the Hamiltonian which couples the two, i.e., the term $-e\mathbf{P}\cdot\mathbf{B}$, where $\mathbf{B}$ is the vector potential operator. As a result of this coupling, the degeneracy is

[7] J. P. Barrat and C. Cohen-Tannoudji, J. Phys. Radium **22**, 329 (1961).

lifted and the levels will have the form shown schematically by the dashed lines 2′ and 3′. Now, transitions from the valence band to the combined states with the absorption of a photon $\hbar\omega$ is possible if there exists a K value for which the difference between the valence-band energy and one of the combined states 2′ or 3′ is equal to $\hbar\omega$. It is easily seen that in the case of positive combined masses [Fig. 7(c)] such a K value always exists, whereas in the case of negative combined masses [Fig. 7(d)] there is a range of values of ω for which the transitions are not allowed.

Numerical computations for the change in $\mathbf{J}_{\omega s}$ caused by the Ω perturbation were carried out for a finite value of T and taking the curvature of the bands into account. The results for $\Delta\mathbf{J}_{\omega s}$ are shown in Fig. 8. Here, $\Delta\mathbf{J}_{\omega s}$ is given as a function of $\hbar\omega$, and γ_{13} as a parameter. At the origin the coordinate $\hbar\omega$ has the value for which a true double-resonance condition exists. For negative values of γ_{13} one indeed observes a very large decrease in $\mathbf{J}_{\omega s}$, although $\mathbf{J}_{\omega s}$ does not go to zero because T is finite. Comparison of $\Delta\mathbf{J}_{\omega s}$ for positive and negative γ_{13} shows that $\Delta\mathbf{J}_{\omega s}$ in the first case is much smaller (2 orders of magnitude) than in the second. The increase in $\Delta\mathbf{J}_{\omega s}$ which appears in Fig. 4 for $\hbar\Omega<\hbar\Omega_{320}$ and $\hbar\omega>\hbar\Omega_{210}$ is therefore seen to be the tail of the double resonance. No such behavior exists in the case of $\gamma_{13}>0$, as seen in Fig. 2. The results of $\Delta\mathbf{J}_{\omega c}$ are given in Fig. 9. These results are, of course, related to those of $\Delta J_{\omega s}$ by the Kramers-Kronig relations.

The general case, where the two surfaces $\hbar\Omega_{21}-\hbar\omega=0$ and $\hbar\Omega_{31}-\hbar(\omega+\Omega)=0$ are not spheres, can now be considered. For a given value of $\hbar\Omega$, the range of $\hbar\omega$ for which the two surfaces just about touch is of particular importance, since one would expect that in this range $\Delta\mathbf{J}_{\omega}$ will strongly vary as a function of $\hbar\omega$. An approximate way of calculating $\Delta\mathbf{J}_{\omega}$ in this case is described in the Appendix. It is found that the form of the spectrum in this case is, except for a factor, identical (within the approximation) to the integral, with respect to $\hbar\omega$ of $\Delta\mathbf{J}_{\omega}$, as computed for the case of the spherical surfaces. One limit of the integration is infinity and the other depends on the value of $\hbar\omega$ at which the value of $\Delta\mathbf{J}_{\omega}$ is being evaluated.

Computed results for $\Delta\mathbf{J}_{\omega}$ in the general case are shown in Figs. 10 and 11. Here, $\Delta\mathbf{J}_{\omega}$ is given as a function of $\hbar\omega$ with ξ_{23} as a parameter. γ_{13} is again negative. For positive γ_{13}, $\Delta\mathbf{J}_{\omega}$ is extremely small. The values of $\Delta J_{\omega}/J_{\omega}$ in this case are four orders of magnitude smaller than in the case of the spherical surfaces computed for equal intensity of the Ω beam. Therefore, observation of this effect will be rather difficult.

IV. PARAMETRIC BEAM

The polarization current at the frequency $\omega+\Omega$ for a given $\mathbf{K}$ value can be singled out from Eq. (18),

$$\mathbf{J}_{0(\omega+\Omega)}=-\frac{eh}{m}\frac{\omega+\Omega}{E_3-E_1}(\rho_{13}\mathbf{P}_{31}+\rho_{31}\mathbf{P}_{13}). \tag{25}$$

Substituting the expression for ρ_{13} given in Eq. (12) we obtain

$$\mathbf{J}_{0(\omega+\Omega)}=\frac{e}{\hbar^2 m}\frac{\hbar(\omega+\Omega)}{E_3-E_1}\left(d_{12}d_{23}\mathbf{P}_{13}\frac{e^{i(\omega+\Omega)t}}{[i(\omega-\Omega_{21})+T^{-1}][i(\omega+\Omega-\Omega_{31})+T^{-1}]+|d_{23}|^2/\hbar^2}+\text{c.c.}\right). \tag{26}$$

The total polarization-current density may be found now by integrating over $\mathbf{K}$ space,

$$\mathbf{J}_{\omega+\Omega}=\frac{1}{4\pi^3}\int_{\text{BZ}} d^3K\,\mathbf{J}_{0(\omega+\Omega)}. \tag{27}$$

As is well known, the polarization-current density vanishes for crystals with inversion symmetry. This can be seen in detail in the following way: We first add up the currents for $\mathbf{K}$ and $-\mathbf{K}$ [notice that $P_{ij}(\mathbf{K})=-P_{ij}{}^*(-\mathbf{K})$] and then integrate over half of the Brillouin zone. The result is found to be

$$\mathbf{J}_{\omega+\Omega}=\frac{1}{4\pi^3}\int_{\text{hBZ}} d^3K\frac{e}{\hbar^2 m}\frac{\hbar(\omega+\Omega)}{E_3-E_1}2\,\text{Im}(d_{12}d_{23}\mathbf{P}_{13}{}^*)\left(\frac{ie^{i(\omega+\Omega)t}}{[i(\omega-\Omega_{21})+T^{-1}][i(\omega+\Omega-\Omega_{31})+T^{-1}]+|d_{23}|^2/\hbar^2}+\text{c.c.}\right). \tag{28}$$

In crystals for which there is inversion, $d_{12}d_{23}P_{13}{}^*$ is always real, thus $\mathbf{J}_{\omega+\Omega}$ vanishes.

The parametric current $\mathbf{J}_{\omega+\Omega}$ produces a beam at this frequency. However, since the photon energy $\hbar(\omega+\Omega)$ is larger than the minimum gap, only the current within the penetration depth of a beam at the frequency $(\omega+\Omega)$ will contribute to the beam emitted from the crystal. Since the penetration depth is less than a wavelength, the intensity of the beam is proportional to the amplitude squared of $\mathbf{J}_{\omega+\Omega}$ and to the square of the penetration depth. The direction in which the beam is emitted is uniquely determined by the incident beams. The direction is such that the projection of the wave number $\mathbf{K}_{\omega+\Omega}$ on the emitting surface is equal to the sum of the components of $\mathbf{K}_{\omega}$ and $\mathbf{K}_{\Omega}$ on the emitting surface.

The amplitude squared of the current density $\mathbf{J}_{\omega+\Omega}$ has been evaluated for the general case in which the

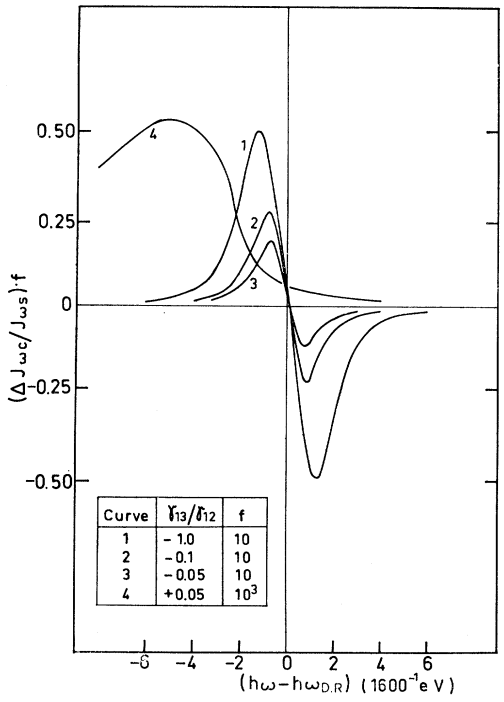

FIG. 9. $\Delta J_{\omega c}/J_{\omega s}$ as a function of the deviation of $\hbar\omega$ from its double-resonance value $\hbar\omega_{DR}$ computed under the following conditions: $T=10^{-12}$ sec; $\hbar\omega_{DR}-\hbar\Omega_{210}=30$ meV; $\xi_{23}=0.5$. (The corresponding intensity of the Ω perturbation is approximately equal to 5×10^7 W/cm^2.) Horizontal coordinate: 1 unit$=1600^{-1}$ eV.

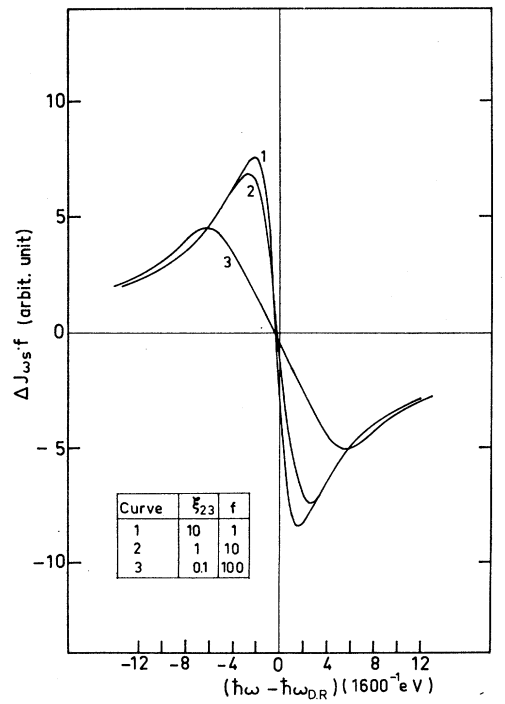

FIG. 10. $\Delta J_{\omega s}$ as a function of $(\hbar\omega-\hbar\omega_{DR})$ for different values of ξ_{23}, computed under the following conditions: $\eta_{31}/\eta_{21}=-1$ and $T=10^{-12}$ sec. Horizontal coordinate: 1 unit$=1600^{-1}$ eV. Vertical unit: arbitrary.

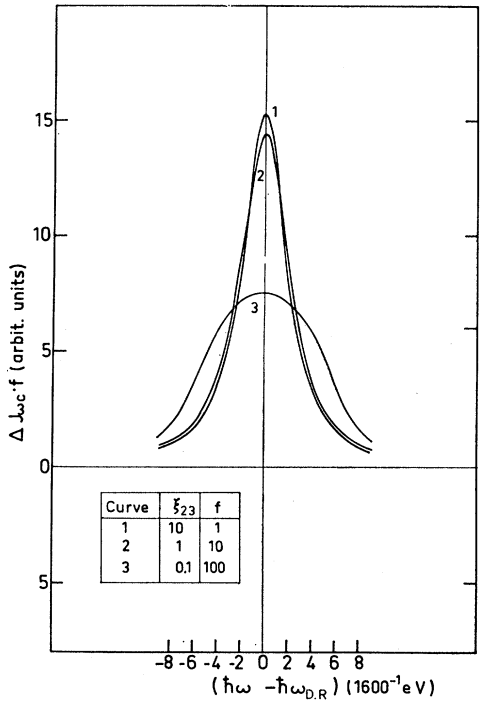

FIG. 11. $\Delta J_{\omega c}$ as a function of $(\hbar\omega-\hbar\omega_{DR})$ for different values of ξ_{23}, computed under the following conditions: $\eta_{31}/\eta_{21}=-1$ and $T=10^{-12}$ sec. Horizontal coordinate: 1 unit$=1600^{-1}$ eV. Vertical unit: same as in Fig. 10.

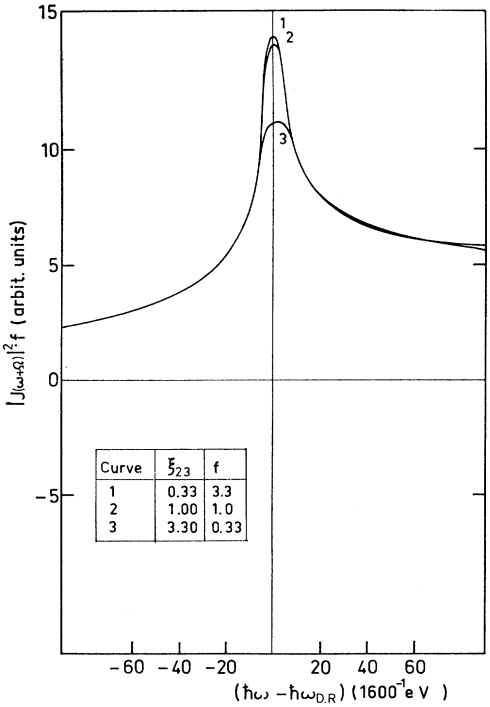

FIG. 12. $|J_{\omega+\Omega}|^2$ as a function of $(\hbar\omega-\hbar\omega_{DR})$ for different values of ξ_{23} computed with $T=10^{-12}$ sec and $\eta_{31}/\eta_{21}=-2$. Horizontal coordinate: 1 unit$=1600^{-1}$ eV. Vertical unit: arbitrary.

surfaces $\hbar\Omega_{31}-\hbar(\omega+\Omega)=0$ and $\hbar\Omega_{21}-\hbar\omega=0$ are not spheres. In this case the integration in K space is performed in just the same way that the current $\mathbf{J}_\omega$ was calculated. Certain insight into the results may be gained if one considers the case where $T\rightarrow\infty$. Close to the point of contact of the two surfaces, one can approximate Ω_{21} and Ω_{31} by the expressions (A3) and (A4) in the Appendix. In performing the integral over K space, we first integrate over $K_\perp$. One easily observes that the integral over $K_\perp$ vanishes if η_{21} and η_{31} have the same sign, whereas it does not always vanish if η_{21} and η_{31} have opposite signs. Thus, a significant parametric beam is expected only in the case that η_{21} and η_{31} have opposite signs. This is just the case when one expects to observe changes in the polarization current $\mathbf{J}_\omega$ caused by the Ω perturbation.

The intensity of the parametric beam as a function of ω for several values of the intensity of the Ω perturbation is given in Fig. 12. It is seen that the intensity of the beam has a peak when the two surfaces in $\mathbf{K}$ space touch. The intensity of the beam is proportional to ξ_{23} and thus to the intensity of the Ω beam, as long as $\xi_{23}<1$. When ξ_{23} becomes larger than unity, the intensity of the parametric beam saturates at the peak. At the peak, the intensity of the parametric beam is about five orders of magnitude smaller than the intensity of the ω beam. This result was obtained when the intensity of the Ω beam was taken to be equal to 10^8 W/cm^2. In order to obtain more definite results one should take a particular band structure and known values for the matrix elements.

V. APPLICATION OF DOUBLE RESONANCE TO INVESTIGATION OF BAND STRUCTURE IN SOLIDS

The strong dependence of double-resonance phenomena on photon energy suggests that one could use them in order to obtain information on the band structure. In discussing the different possibilities, let us consider two cases:

Case a. Double-resonance conditions take place in the vicinity of the point in K space at which all the bands have extrema.

The change in the polarization currents at the ω frequency $\Delta\mathbf{J}_\omega$, as a function of $\hbar\omega$, shows pronounced structure centered around the point $\hbar\omega=\hbar\Omega_{210}$. The width of the peaks are of the order of a few meV. Thus, measurement of $\Delta\mathbf{J}_\omega$, as a function of $\hbar\omega$ will allow one to determine quite precisely the value of the energy gap $\hbar\Omega_{210}$. This information is actually of the same kind that one obtains in ordinary differential measurements, except that in this case the varying parameter is the laser light. As can be seen, $\Delta\mathbf{J}_\omega$ varies quite drastically as one approaches the point at which $\hbar\Omega=\hbar\Omega_{320}$. Therefore, measurement of $\Delta\mathbf{J}_\omega$ as a function of $\hbar\omega$ for different values of $\hbar\Omega$ will allow one to determine $\hbar\Omega_{320}$. In the computation presented in Sec. IV, we assumed that the matrix elements $\mathbf{P}_{12}$ and $\mathbf{P}_{23}$ do not vanish. This condition is complementary in many cases to the condition $\mathbf{P}_{13}\neq 0$, which is necessary in order to obtain the information about band 3 by the electroreflectance methods.

Certain remarks about the actual performance of the measurements should be brought out here:

(1) It is necessary to use a laser with frequency that can be changed continuously over a wide range. Dye lasers appear to be most appropriate.

(2) These experiments may be performed only on materials for which $\hbar\Omega_{320}$ is smaller than the minimum energy gap, and in addition the transition from 2 to 3 is allowed.

Case b. Double resonance occurs at photon energies $\hbar\omega$, which correspond to a nonextremal gap between the valence and a conduction band. In this case, one obtains a well-defined structure in the spectra of $\Delta\mathbf{J}_\omega$ and of the parametric beam close to the point at which the two surfaces ($\hbar\Omega=\hbar\Omega_{32}$ and $\hbar\omega=\hbar\Omega_{21}$) touch or coincide.

Measurement of ΔJ_ω as a function of $\hbar\omega$ or measurement of the intensity of the parametric beam as a function of $\hbar\omega$ will yield two energies $\hbar\omega$ and $\hbar\Omega$ which are equal to $\hbar\Omega_{21}$ and $\hbar\Omega_{32}$ corresponding to the same $\mathbf{K}$ value in the Brillouin zone. We also know that the two surfaces will, in general, touch at points which lie along lines of high symmetry in $\mathbf{K}$ space. These lines can in most cases be determined with only a rough knowledge of the band structure. One can use this information in two ways:

(1) Knowledge of the effective masses of the valence and lower conduction band from other measurements and knowledge of $\hbar\Omega_{32}$ as a function of $\hbar\Omega_{21}$ from the double-resonance measurement allows one to determine the unknown effective mass of the upper conduction band.

(2) Direct comparison of the experimental results with theory can be done in the following way. One can determine the value of K along the proper high-symmetry line for which $\hbar\Omega_{32}=\hbar\Omega$ and check at that same $\mathbf{K}$ value how well the theoretical value of $\hbar\Omega_{21}$ compares with the experimental value of $\hbar\omega$. Use of polarized light will provide information about the symmetry properties of the bands along the lines of high symmetry.

We would like to emphasize several points about the double-resonance experiments discussed here.

(1) The effects are strong only when at the point of contact of the two surfaces in K space $\hbar\Omega_{31}$ increases when $\hbar\Omega_{21}$ decreases or vice versa.

(2) It is necessary that $\hbar\Omega$ be smaller than the minimum energy gap.

(3) In the case of a crystal which does not have inversion symmetry, it will be easier to observe the

parametric beam rather than the variation of the reflection coefficient of the monochromatic beam.

In conclusion, two nonlinear optical effects were considered under double-resonance conditions in a solid. Measurement of these effects has been shown to give information complementary to the information obtained by other optical methods. In addition, it may give new information about noncritical points in the Brillouin zone which cannot be obtained by other methods. Additional double-resonance effects may be of interest, such as effects associated with excitons.

ACKNOWLEDGMENTS

It is a pleasure to thank Professor S. Yatsiv for many useful discussions. Professor Yatsiv's work on nonlinear optical phenomena in gases was indeed the first stimulant to this work. I also thank Professor Low for his interest in this work and for many enlightening discussions on the subject.

APPENDIX: EVALUATION OF POLARIZATION CURRENT IN GENERAL CASE

The evaluation of $\mathbf{J}$ is carried out for values of ω and Ω which are close to the values for which the surfaces $\hbar\Omega_{21}-\hbar\omega=0$ and $\hbar\Omega_{31}-\hbar(\omega+\Omega)=0$ touch. The total change in the polarization current $\Delta\mathbf{J}$ is given by

$$\Delta\mathbf{J}=\frac{1}{4\pi^3}\int\int\int\Delta\mathbf{J}_0\,d^3K. \tag{A1}$$

The main contribution to this integral comes from the region around the points of contact of the two surfaces. We therefore define the following coordinate system. For a given value of Ω the point at which the two surfaces touch is taken as the origin. Then $K_\perp$ is the coordinate perpendicular to the surfaces at the point of contact and $\mathbf{K}_s$ is a vector in the plane tangent to the two surfaces. Thus,

$$\Delta\mathbf{J}=\frac{1}{4\pi^3}\sum_n\int\int d^2K_s\int\Delta\mathbf{J}_0 dK_\perp. \tag{A2}$$

The sum is over all points of contact. $\Delta\mathbf{J}_0$ depends on $K_\perp$ and on $\mathbf{K}_s$ through $\omega-\Omega_{21}$ and $\omega+\Omega-\Omega_{31}$. Notice that ξ_{23} does not vary appreciably around a point of contact but will vary from one point of contact to another. In the vicinity of a point of contact Ω_{21} and Ω_{31} may be expanded in the following way:

$$\Omega_{21}=\Omega_{21c}+F_{21}(\mathbf{K}_s)+\eta_{21}K_\perp, \tag{A3}$$

$$\Omega_{31}=\Omega_{31c}+F_{31}(\mathbf{K}_s)+\eta_{31}K_\perp, \tag{A4}$$

where $\hbar\Omega_{21c}$ and $\hbar\Omega_{31c}$ are the energy gaps between bands 2 and 1 and between bands 3 and 1, respectively, at the point of contact. Thus, $\Omega_{31c}-\Omega_{21c}=\Omega$. From this we find the following relations:

$$(\omega-\Omega_{21})/\eta_{21}=(\omega-\Omega_{21c})/\eta_{21}-F_{21}(\mathbf{K}_s)/\eta_{21}-K_\perp, \tag{A5}$$

$$(\omega+\Omega-\Omega_{31})/\eta_{31}=(\omega-\Omega_{21c})/\eta_{31}-F_{31}(\mathbf{K}_s)/\eta_{31}-K_\perp. \tag{A6}$$

Since $\Delta\mathbf{J}_0$ approaches zero far away from the point of contact, the integration with respect to $K_\perp$ may be carried out from $-\infty$ to ∞. As a result of this $\Delta\mathbf{J}_1$, the integral of $\Delta\mathbf{J}_0$ with respect to $K_\perp$ depends on ω and $\mathbf{K}_s$ through the difference $\Delta\Omega'$,

$$\Delta\Omega'=(\omega-\Omega_{21c})\left(\frac{1}{\eta_{21}}-\frac{1}{\eta_{31}}\right)+\frac{F_{31}(\mathbf{K}_s)}{\eta_{31}}-\frac{F_{21}(\mathbf{K}_s)}{\eta_{21}}. \tag{A7}$$

Since η_{21} and η_{31} are constant, we define for reasons of convenience another variable $\Delta\Omega$:

$$\Delta\Omega=\Delta\Omega'/(\eta_{21}^{-1}-\eta_{31}^{-1}). \tag{A8}$$

$F_{21}(\mathbf{K}_s)$ and $F_{31}(\mathbf{K}_s)$ are quadratic in $\mathbf{K}_s$. Thus, choosing proper coordinates K_{s1} and K_{s2}, one can express $\Delta\Omega$ in the following way:

$$\Delta\Omega=(\omega-\Omega_{21c})\pm(K_{s1}^2/S_1^2+K_{s2}^2/S_2^2). \tag{A9}$$

S_1, S_2, and the sign are determined by the band structure of the material. Using this relation the variables of integration K_{s1} and K_{s2} may be changed to the variable $\Delta\Omega$. We then obtain

$$\Delta\mathbf{J}=\pm\sum_n\pi S_1S_2\int_{\omega-\Omega_{21c}}^{\pm\infty}\Delta\mathbf{J}_1\,d\Delta\Omega. \tag{A10}$$

Notice that $\Delta J_{\omega 1}$ as a function of $\Delta\Omega$ is to within a constant factor equal to $\Delta\mathbf{J}_\omega(\omega)$ as computed in the case of spherical surfaces (assuming the dependency of Ω_{21} and Ω_{31} on $K_\perp$ is linear). It is therefore seen that $\Delta\mathbf{J}_\omega$ in the general case is given to within a constant factor by an integral with respect to ω of $\Delta\mathbf{J}_\omega$ as computed in the spherical case.